Materials Advances

ROYAL SOCIETY OF CHEMISTRY

PAPER

View Article Online
View Journal | View Issue

Cite this: *Mater. Adv.*, 2026, 7, 3576

The glass transition width and its dependence on fragility, nonexponentiality and nonlinearity

Jiří Málek

Received 16th December 2025,
Accepted 14th March 2026

DOI: 10.1039/d5ma01473e

rsc.li/materials-advances

This paper presents a comprehensive and critical analysis of the glass transition width $\left(1/T_g - 1/T'_g\right)$ or the reduced width $\left(\Delta T_g/T'_g\right)$ observed in simulated differential scanning calorimetry (DSC) heating and cooling scans. The study employs the Tool-Narayanaswamy-Moynihan model (TNM) for 24 diverse materials, encompassing inorganic glasses, organic polymers and molecular glassy systems. The analysis reveals an important novel finding. The width (or the reduced width) of the glass transition cooling scan is shown to be inversely proportional to the activation energy (h^*/R), or fragility index (m), as well as the sum the non-exponentiality β and nonlinearity x parameters, following the relationship: $[(h^*/R) \times (\beta + x)]^{-1}$ or $[m \times (\beta + x)]^{-1}$. With precise determinations of T_g and T'_g, the estimated sum of $(\beta + x)$ achieves an accuracy comparable to Hutchinson's established peak shift method.

1. Introduction

The glass transition, defined as the continuous transformation of a supercooled liquid into a glassy state upon cooling to sufficiently low temperatures, is an essential feature of all glassy materials, including organic polymers, oxides, chalcogenides, metallic alloys, and molecular systems. This phenomenon is primarily kinetic; nonetheless, it exhibits distinct thermodynamic characteristics – such as a step change in heat capacity or thermal expansion coefficient – resulting from the loss of configurational degrees of freedom as molecular motion is arrested.

Over 30 years ago, Moynihan's work[1] established a correlation between the width of the glass transition region (as measured by Differential Scanning Calorimetry, DSC) and the activation energy (h^*/R) for the structural relaxation of high-T_g inorganic glasses. Moynihan defined a dimensionless parameter, C, as a constant specific to certain inorganic glasses.[1,2] This parameter is derived from the reciprocal temperatures at the onset $(1/T_g)$ and end $\left(1/T'_g\right)$ of the glass transition on a DSC thermogram:

$$\left(\frac{h^*}{R}\right) \times \left(\frac{1}{T_g} - \frac{1}{T'_g}\right) = C \qquad (1)$$

The eqn (1) is valid provided that the ratio of cooling to heating rates $|q_c/q_h|$ remains fixed. Moynihan[1] also determined that T_g and T'_g for a given glass remain invariant, within experimental error, as long as the cooling/heating rate ratio stays within the range of 0.2 to 5. This correlation was later extended to molecular glasses by combining DSC and dielectric relaxation data and utilizing the $F_{1/2}$ fragilities.[3]

However, this extension of the Moynihan correlation has been challenged. Johari *et al.*[4] used simulations to show that a simple relationship between the DSC endotherm width and the non-Arrhenius temperature dependence of a liquid's kinetic property requires explicitly including the distribution of relaxation times. The method's general applicability was further questioned by Hancock *et al.*,[5] who tested it on various pharmaceutical glass-forming materials. They concluded that the conditions required for eqn (1) to be universally applicable with a constant C are not met for a wide range of glassy materials.

Pikal *et al.*[6] later provided a detailed analysis of experimental data for (poly)vinyl pyrrolidone, sucrose, and trehalose. Their approach, which combined various experimental procedures combined with simulations of theoretical curves, was equivalent to the comprehensive Tool-Narayanaswamy-Moynihan (TNM) formalism. Within this work, Pikal *et al.* found that a modification of Moynihan's original equation provides a much better correlation for both their experimental and simulated data.[6] This modified equation incorporates the stretched exponential parameter β (a measure of non-exponentiality) to more accurately describe the relaxation behaviour of these glassy materials. They reformulated eqn (1) to account for this non-exponentiality:

$$\beta \times \left(\frac{h^*}{RT_g}\right) = \frac{C'}{\Delta T_g/T_g} \qquad (2)$$

In this equation, $\Delta T_g = T'_g - T_g$ and C' is a constant.

Department of Physical Chemistry, Faculty of Chemical Technology, University of Pardubice, Studentská 573, Pardubice 532 10, Czech Republic.
E-mail: jiri.malek@upce.cz

Building on this, Chen *et al.*[7] reported that the reduced glass transition width, $\Delta T_g/T_g$, is influenced by the fragility index, $m = (h^*/RT_g)/\ln(10)$, and the stretched exponential parameter, β. In contrast, they found no significant relationship between the nonlinearity parameter (x of the TNM model) and $\Delta T_g/T_g$. More recently, Bogdanova and Kocherbitov[8] applied this formalism to a sucrose–water system and arrived at very similar conclusions, corroborating the findings of Chen *et al.* This convergence suggests that the relationship between fragility, non-exponentiality, and the width of the glass transition may hold for a broader class of glassy materials.

In his seminal papers,[9,10] Donth utilized the glass transition width determined from DSC thermograms even earlier than the aforementioned studies.[1–8] By assuming mean temperature fluctuation within cooperatively rearranging regions (CRRs), Donth proposed a method to estimate average size of these thermodynamic subsystems based on the shape of thermal relaxation spectrum. This approach has since been applied to the analysis of conventional, modulated, and fast DSC data for polymers, a-Se,[11] and metallic glasses.[12] Recently, Schawe *et al.*,[13] compared the characteristic length of dynamic heterogeneities across a wide range of glass-formers. Their work discussed the correlation between chemical structure, the size of dynamic heterogeneities, and the macroscopic kinetics of the glass transition, revealing nearly universal behaviour among studied systems.

Previous studies[1–8] were restricted to analyzing heating DSC curves, typically measured or simulated immediately after a prior cooling from equilibrium supercooled liquid well above the glass transition. This paper provides a comprehensive and critical analysis of the glass transition width within a DSC thermal cycle, utilizing simulated cooling and subsequent heating curves based on TNM parameters for 24 diverse materials, including inorganic glasses to organic polymers and some molecular systems. The results indicate that the width of the cooling DSC curve exhibits an inverse proportionality to the material's fragility and to the combined sum of the non-exponentiality (β) and nonlinearity (x) parameters.

2. The TNM model

The Tool-Narayanaswamy-Moynihan (TNM) formalism, an important model for structural relaxation in glassy materials, integrates three fundamental concepts. The first concept, introduced by Tool,[14,15] posits that relaxation time depends on both temperature T and the material's actual structure, represented by the fictive temperature T_f. The fictive temperature essentially defines the temperature at which an equilibrium supercooled liquid would possess the same structure as the non-equilibrium glass. It is defined by an empirical equation

$$\tau(T, T_f) = A \cdot \exp\left[x\frac{h^*}{RT} + (1-x)\frac{h^*}{RT_f}\right] \quad (3a)$$

where $0 < x \leq 1$ is the nonlinearity parameter, h^*/R is the effective activation energy and A is an adjustable parameter. An alternative approach provides a natural separation of T and T_f. Building on the Adam–Gibbs[16] cooperative relaxation theory, Hodge[17] derived the following expression for relaxation time:

$$\tau(T, T_f) = \tau_0 \exp\left[\frac{Q}{T(1 - T_2/T_f)}\right] \quad (3b)$$

where τ_0 is a constant and $Q = N_A s^* \Delta\mu / k_B C$. In the Adam–Gibbs theory, s^* and $\Delta\mu$ represent the minimum entropy required for rearrangement and the activation energy for a single rearrangement, respectively. The parameter T_2 is conceptually similar to the Fulcher or Kauzmann temperature and C is the extrapolated value of the configurational heat capacity at that temperature. In the equilibrium state above the glass transition where $T_f = T$, eqn (3b) reduces to the Vogel–Fulcher–Tammann equation with $T_0 = T_2$. Comparing eqn (3a) and (3b), the nonlinearity can be expressed as $T_2/T_g \cong (1 - x)$.

The second essential concept was introduced by Narayanaswamy.[18] According to his model, the structural relaxation should be linear in terms of the material (or reduced) time defined by

$$\xi = \int_0^t \frac{dt}{\tau(T, T_f)} \quad (4)$$

Material time quantifies how fast individual processes take place during physical aging, effectively reflecting the existence of a material 'inner clock.' While Dyre[19] later utilized the nonlinear fluctuation-dissipation theorem to derive the TNM phenomenological theory and suggested a pathway connecting this concept with material time in rheology, it is interesting to note that Hopkins[20] proposed a similar concept for stress relaxation in viscoelastic substances under varying temperature even earlier than the Narayanaswamy's seminal paper. More recently, Douglas and Dyre[21] have suggested that the inherent harmonic mean-square displacement – which emphasizes the behaviour of the slowest-moving particles – is likely the key quantity controlling material time.

The third fundamental concept integrates Tool's fictive temperature with the material-time concept. Mazurin *et al.*[22] and Moynihan *et al.*,[23,24] employed the stretched exponential function, ϕ, to account for the nonexponentiality of the structural relaxation, as shown in eqn (5).

$$\phi = \exp(-\xi^\beta) \quad (5)$$

In this equation, the non-exponentiality parameter $0 < \beta \leq 1$ is inversely proportional to the width of the distribution of relaxation times. Together, eqn (3a), (4), and (5) fully constitute the Tool-Narayanaswamy-Moynihan formalism, a cornerstone model for understanding structural relaxation in glassy materials.[23,24]

3. Simulation of DSC curves in the glass transition range

The structural relaxation is usually simulated in terms of evolution of the fictive temperature for a well-defined time-

temperature protocol. This protocol captures the entire thermal history of a glassy material from the very first moment of its departure from metastable equilibrium supercooled liquid well above the glass transition. The structural relaxation can be described by combining the material-time concept (eqn (4)), and the Boltzmann superposition principle for any given time-temperature protocol.[24]

For practical implementation, the protocol is often discretized into several consecutive steps, which may involve a heating/cooling ramp or isothermal annealing. For the TNM model, the evolution of the fictive temperature during continuous heating or cooling at a constant rate $q_k = \mathrm{d}T/\mathrm{d}t$ (negative for cooling) then can be expressed[22] by eqn (6a) and (6b):

$$T_\mathrm{f} = T_\mathrm{ini} - \sum_{j=1}^{n} \Delta T_j \left\{ 1 - \exp\left[-\left(\sum_{k=j}^{n} \frac{\Delta T_k}{q_k \tau_k} \right)^{\beta} \right] \right\} \tag{6a}$$

$$\tau_k = A \cdot \exp\left[x \frac{h^*}{RT_k} + (1-x) \frac{h^*}{RT_{\mathrm{f},k-1}} \right] \tag{6b}$$

where T_ini is the initial temperature corresponding to the metastable equilibrium supercooled liquid, where $T_\mathrm{f}(T_\mathrm{ini}) = T_\mathrm{ini}$. Eqn (6a) represents an implicit function for the relaxation time τ_k, as its expression depends on the function's value itself – specifically, the fictive temperature at the end of the previous step, $T_{\mathrm{f},k-1}$. The heating or cooling experiment is modelled using small discrete temperature steps, $\Delta T_k \approx 100$ mK, with the fictive temperature calculated iteratively at the end of each temperature step, using eqn (6a) and (6b). To maintain linearity within these subintervals, ΔT_k must be sufficiently small that T_f decays by less than approximately 100 mK between steps. The temperature derivative of the fictive temperature $\mathrm{d}T_\mathrm{f}/\mathrm{d}T$ following the n-th step is obtained from the following equation[24]

$$\left(\frac{\mathrm{d}T_\mathrm{f}}{\mathrm{d}T} \right)_n = \frac{T_{\mathrm{f},n} - T_{\mathrm{f},n-1}}{\Delta T_n} \tag{7}$$

Fig. 1b shows a thermal cycle, illustrating the simulated cooling (#1) and subsequent heating (#2) curves from eqn (6) and (7) using an identical scanning rate $q = \pm 10$ K min^{-1}. The cooling ($\mathrm{d}T_\mathrm{f}/\mathrm{d}T$) curve exhibits a simple sigmoidal shape, contrasting sharply with the more complicated heating curve, which features kinetic phenomena such as a minimum (undershoot) and maximum (overshoot). Fig. 1a clearly indicates that the limiting fictive temperature T_lim is identical for both scans – a characteristic result for this type of thermal cycle. T_lim is situated close to the inflectional point of the cooling curve and the extrapolated onset of the heating curve (T_g).

The derivative $\mathrm{d}T_\mathrm{f}/\mathrm{d}T$ in fact corresponds to the heat capacity C_p^N, which is equivalent to a DSC curve scaled between 0 and 1:

$$C_\mathrm{p}^N = \frac{(C_\mathrm{p} - C_\mathrm{pg})|_T}{(C_\mathrm{pl} - C_\mathrm{pg})|_{T_\mathrm{f}}} = \frac{\mathrm{d}T_\mathrm{f}}{\mathrm{d}T} \tag{8}$$

where C_pg and C_pl are heat capacities of the glass and supercooled liquid, respectively. Any experimental DSC data can easily be converted to C_p^N *versus* T dependence by using the eqn (8).

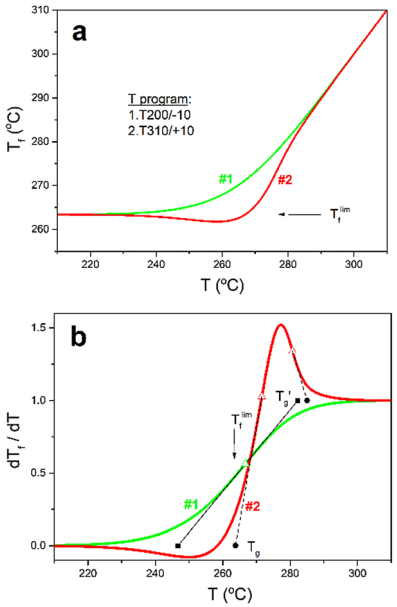

Fig. 1 The fictive temperature T_f and its derivative $\mathrm{d}T_\mathrm{f}/\mathrm{d}T$, calculated using eqn (6) and (7) for the TNM parameters: h^*/R = 51.2 kK, ln(A/s) = 90.8, x = 0.96, β = 0.84. The temperature program used was T_ini = 310 °C, q_c = −10 K min^{-1}, q_h = +10 K min^{-1}. Open triangles mark inflection points. Full circles and full squares indicate the extrapolated inflectional tangent intersection with $\mathrm{d}T_\mathrm{f}/\mathrm{d}T$ = 0 and $\mathrm{d}T_\mathrm{f}/\mathrm{d}T$ = 1 lines, respectively. Inflectional tangents for heating data are represented by dashed lines, while those for cooling data use solid line. Arrow indicates limiting fictive temperature.

To demarcate the lower end of the glass transition region for DSC heating curve Moynihan[1] used "extrapolated temperature of onset of rapid rise of the C_p *vs.* T curve, T_g", as shown in Fig. 1b. To demarcate upper end of the glass transition for heating DSC data "the extrapolated temperature of completion of the overshoot, T_g' was used." However, this manual approach is inadequate for the precise numerical analysis of simulated DSC data. To overcome this limitation, we propose a refined numerical procedure. Step 1: the inflection points of the simulated DSC heating data are first determined numerically; step 2: tangents are then calculated at these inflection points using linear regression, based on 10 to 20 adjacent data points to ensure a correlation coefficient greater than 0.9999; step 3: the intersections of these tangents define the characteristic temperatures: T_g is the intersection with $\mathrm{d}T_\mathrm{f}/\mathrm{d}T = 0$, and T_g' is the intersection with $\mathrm{d}T_\mathrm{f}/\mathrm{d}T = 1$. The dashed lines in Fig. 1b illustrate this; the same procedure was similarly employed for the analysis of simulated DSC cooling data, which is represented by the solid line in Fig. 1b.

4. Results and discussion

Table 1 presents a selection of previously reported Tool-Narayanaswamy-Moynihan (TNM) parameter sets for 24 diverse materials, encompassing a wide range of properties. The

Table 1 The TNM parameters for selected non-crystalline materials reported in literature[17,24–43]

Material	h^*/R [kK]	$-\ln(A/s)$	x	β	Ref.
PVC	225.0	622.0	0.10	0.23	17
PMMA	138.0	357.8	0.19	0.35	17
PS bulk	83.4	212.5	0.18	0.43	25
ZBLA	165.0	282.6	0.19	0.50	26
$Li_2O{\cdot}SiO_2$	111.8	150.8	0.27	0.48	27
PC	150.0	353.6	0.22	0.54	28
Glycerol	16.0	81.0	0.29	0.51	29
EG gel	12.0	75.5	0.46	0.39	26
PVAc	71.3	223.6	0.35	0.57	30
PS	126.6	334.7	0.29	0.69	31
Se	42.8	133.0	0.42	0.58	32
TPD bulk	109.5	321.0	0.64	0.37	33
B_2O_3	45.0	75.6	0.40	0.65	24
LiCl gel	12.0	70.5	0.67	0.39	26
ASAHI plate glass	73.0	83.8	0.45	0.62	34
As_2S_3	32.4	62.1	0.31	0.82	35
$Se_{70}Te_{30}$	34.5	100.0	0.43	0.73	36
As_2Se_3	41.0	85.5	0.49	0.67	37
$(GeSe_2)_{30}(Sb_2Se_3)_{70}$	62.1	120.0	0.52	0.67	38
$(GeS_2)_{30}(Sb_2S_3)_{70}$	60.2	113.0	0.57	0.72	39
NBS711	45.0	57.4	0.65	0.65	40
P-SK57	82.2	101.5	0.75	0.77	41
$(GeS_2)_{50}(Sb_2S_3)_{50}$	51.2	90.8	0.75	0.86	42
$(GeTe_4)_{60}(GaTe_3)_{40}$	40.9	91.9	0.96	0.84	43

apparent activation energies of these materials span from 12 to 225 kK. Similarly, the nonlinearity parameter x varies from 0.10 to 0.96, and the non-exponentiality parameter β ranges from 0.23 to 0.86. This broad range ensures a comprehensive test of validity of the eqn (1) and (2) across different material types.

A complete DSC thermal cycle, – specifically, cooling scan #1 (-10 K min^{-1}) from the equilibrium supercooled liquid at T_{ini} to a temperature well below T_g, followed by subsequent heating scan #2 (+10 K min^{-1}) back to T_{ini} – was calculated using eqn (6) and (7) for all TNM parameter sets listed in Table 1 (see SI). These simulated curves are analyzed separately in the following sections.

4.1. Analysis of simulated DSC heating scans

Moynihan's proposed eqn (1) suggests that $\Delta(1/T_g) = 1/T_g - 1/T_g'$, derived from simulated DSC heating scans (+10 K min^{-1}), multiplied by the reduced activation energy of structural relaxation h^*/R, should equal a constant parameter, C. However, our analysis of 24 diverse materials from Table 1 demonstrates that C depends on the non-exponentiality parameter β (Fig. 2a), a finding previously observed by several authors.[6–8] For the specific range of β the values of C approximate Moynihan's proposed constant ($C \cong 4.8$).[1]

Eqn (1) can thus be reformulated into a different form

$$\Delta(1/T_g)_h = \frac{D}{(h^*/R) \times \beta} \quad (9)$$

that resembles eqn (2) proposed by Pikal *et al.*[6] A plot of $\Delta(1/T_g)_h$ *vs.* $[\beta(h^*/R)]^{-1}$ should produce a straight line passing through the origin, with a slope equal to D, as illustrated in Fig. 2b. Linear regression confirms this relationship, yielding a proportionality constant D of 3.69 ± 0.06 (R^2 = 0.993).

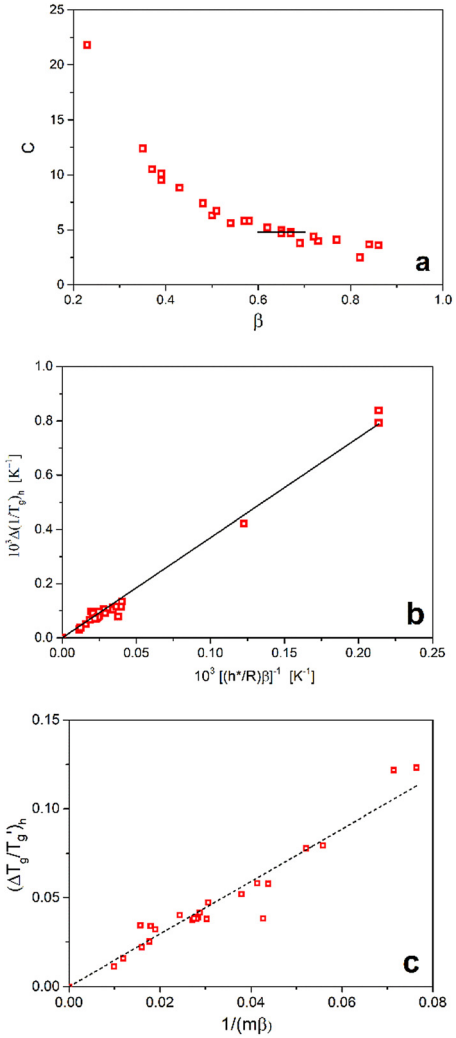

Fig. 2 Analysis of heating DSC scans (q_h = +10 K min^{-1}) following cooling from equilibrium supercooled liquid (q_c = −10 K min^{-1}), simulated using the TNM parameters from Table 1 (points). (a) Dependence of parameter C (eqn (1)) on β. (b) Glass transition width (eqn (9)) as a function of $[(h^*/R) \times \beta]^{-1}$. (c) Reduced glass transition width (eqn (10)) as a function of $[m \times \beta]^{-1}$. Solid and dashed lines represent linear regressions, with slopes D = 3.69 ± 0.06 and D' = 1.48 ± 0.04, respectively.

Alternatively, the reduced glass transition width can be expressed $\left(\Delta T_g/T_g'\right)_h = \left(T_g' - T_g\right)/T_g'$. Eqn (1) can then be rewritten in the following form

$$\left(\frac{\Delta T_g}{T_g'}\right)_h = \frac{D'}{m \times \beta} \quad (10)$$

where m is the fragility index and $D' \cong D/\ln(10)$. The fragility index in this study is defined as $m = (h^*/RT_g)/\ln(10)$, although alternative definitions of fragility have recently been discussed in the literature.[44] A plot of $\left(\Delta T_g/T_g'\right)_h$ *vs.* $[m \times \beta]^{-1}$ should yield a straight line passing through the origin (Fig. 2c). Linear regression validates this relationship, with the proportionality constant D' found to be 1.48 ± 0.04 (R^2 = 0.980).

4.2. Analysis of simulated DSC cooling scans

A similar relationship to eqn (1) can be assumed for cooling DSC scans

$$\left(\frac{h^*}{R}\right) \times \left(\frac{1}{T_g} - \frac{1}{T'_g}\right) = E \qquad (11)$$

The determination of T_g and T'_g followed the procedure detailed in Section 3. The inflection point was first calculated numerically from the simulated DSC cooling data. A tangent was then fitted to this point *via* linear regression of twenty nearest data points, ensuring a correlation coefficient better than 0.9999. As illustrated by a solid line in Fig. 1b, T_g and T'_g are defined by the intersection of this tangent line with $dT_f/dT = 0$ and $dT_f/dT = 1$, respectively.

In contrast to the heating scan analysis, Fig. 3a illustrates that the parameter E for cooling process is dependent on the sum of both nonexponentiality and nonlinearity parameters, specifically $(\beta + x)$. Consequently, eqn (11) can be rewritten as

$$\Delta(1/T_g)_c = \frac{F}{(h^*/R) \times (\beta + x)} \qquad (12)$$

Thus, a plot of $\Delta(1/T_g)_c$ *vs.* $[(h^*/R) \times (\beta + x)]^{-1}$ is expected to yield a straight line that passes through the origin (Fig. 3b). The proportionality constant F, determined *via* linear regression, is 9.7 ± 0.2 ($R^2 = 0.992$).

Similarly, mirroring the observation for the heating scan, the reduced glass transition width for cooling can be expressed as

$$\left(\frac{\Delta T_g}{T'_g}\right)_c = \frac{F'}{m \times (\beta + x)} \qquad (13)$$

where $m = (h^*/RT_g)/\ln(10)$ is the fragility index and $F' \cong F/\ln(10)$. A corresponding plot of $\left(\Delta T_g/T'_g\right)_c$ *versus* $[m\times(\beta + x)]^{-1}$ should also produce a straight line passing through the origin (Fig. 3c). The proportionality constant F' found by this linear regression is 4.10 ± 0.07 ($R^2 = 0.992$).

If the glass transition width $\Delta(1/T_g)_c$ is obtained from the cooling scan, eqn (12) can potentially be used to estimate the value of the sum $(\beta + x)$, provided the activation energy is known. However, such an estimated value is often distorted (usually overestimated), carrying an error margin of about 0.2. Very similar results are obtained when applying eqn (13). Applying the same procedure to heating scans provides even less reliable results; the error margins for the values of β obtained from eqn (9) and (10) exceed 0.2. The primary challenge across all these estimations lies in the uncertainties associated with the accurate determination of $\Delta(1/T_g)_h$ and $\left(\Delta T_g/T'_g\right)_h$. It appears that even the modified procedure detailed earlier in this paper does not provide satisfactory results for accurately determining the nonexponentiality and nonlinearity parameters.

As already pointed out by Johari *et al.*,[4] it is advantageous to use a more self-consistent method for determining $\Delta(1/T_g)$ and $\Delta T_g/T'_g$. In this approach, T_g is defined as the temperature at which the normalized heat capacity ($C_p^N \equiv dT_f/dT$) equals a specific value z. Subsequently, T'_g is determined as the temperature where the normalized heat capacity reaches a value $1 - z$. Fig. 4 illustrates this determination for DSC cooling scans at different scanning rates calculated for PVC and As_2S_3.

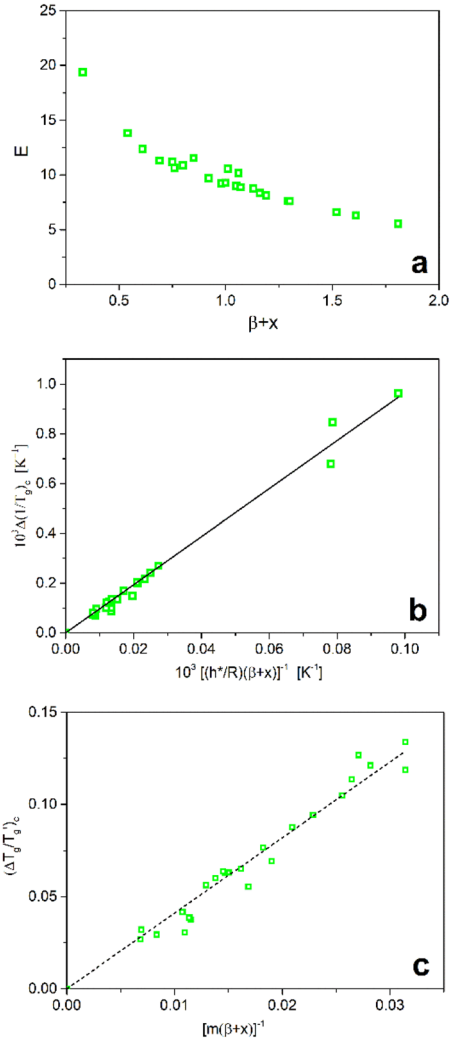

Fig. 3 Analysis of cooling DSC scans ($q_c = -10$ K min^{-1}) from equilibrium supercooled liquid, simulated using the TNM parameters from Table 1 (points). (a) Dependence of parameter E (eqn (11)) on $(\beta + x)$. (b) Glass transition width (eqn (12)) as a function of $[(h^*/R) \times (\beta + x)]^{-1}$. (c) Reduced glass transition width (eqn (13)) as a function of $[m \times (\beta + x)]^{-1}$. Solid and dashed lines represent linear regressions, with slopes $F = 9.7 \pm 0.2$ and $F' = 4.10 \pm 0.07$, respectively.

Fig. 5a represents a plot of $\Delta(1/T_g)_c$ *versus* $[(h^*/R) \times (\beta + x)]^{-1}$, determined using DSC cooling scan at -10 K min^{-1} and a value $z = 0.15$ for all TNM parameter sets listed in Table 1. Linear regression of this data yields the proportionality constant $F = 9.33 \pm 0.05$ ($R^2 = 0.999$). Similarly, Fig. 5b shows a plot of $\left(\Delta T_g/T'_g\right)_c$ *versus* $[m\times(\beta + x)]^{-1}$ for the same TNM parameter sets and z value. The resulting proportionality constant F' is 3.98 ± 0.03 ($R^2 = 0.998$). These dimensionless constants, F and

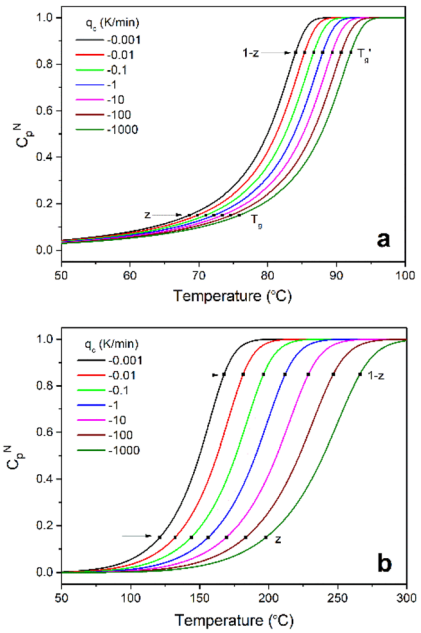

Fig. 4 Determination of the T_g and T_g' (for z = 0.15) from simulated cooling DSC scans for PVC (a) and As_2S_3 (b). Curves are shown for various scanning rates using TNM parameters listed in Table 1.

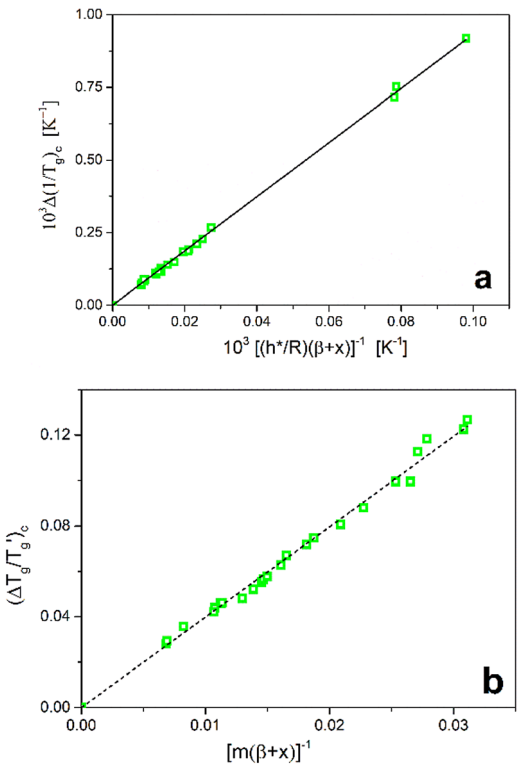

Fig. 5 Analysis of simulated cooling DSC scans (q_c = −10 K min^{-1}) using TNM parameters from Table 1 (points). (a) Glass transition width defined by eqn (12). (b) Reduced glass transition width defined by eqn (13). Lines represent linear fits with F = 9.33 ± 0.05 (solid line) and F' = 3.98 ± 0.03 (dashed line). T_g and T_g' values were determined using the procedure defined in Fig. 4 with z = 0.15.

Table 2 The proportionality constants defined by eqn (12) and (13), determined for various values of parameter z as illustrated in Fig. 4

z	F	F'
0.01	25.2 ± 0.4	10.8 ± 0.3
0.05	16.1 ± 0.1	6.9 ± 0.1
0.10	11.89 ± 0.06	5.08 ± 0.05
0.15	9.33 ± 0.05	3.98 ± 0.03
0.20	7.39 ± 0.04	3.15 ± 0.02
0.25	5.84 ± 0.04	2.49 ± 0.02
0.30	4.45 ± 0.03	1.90 ± 0.01
0.35	3.24 ± 0.03	1.38 ± 0.01
0.40	2.13 ± 0.02	0.904 ± 0.008

$F' \cong F/\ln(10)$ are invariant across different cooling rates and TNM parameter sets. They solely depend on quantity z that has been used for their determination. Table 2 provides their values for selected values of z.

4.3. Estimation of nonexponentiality and nonlinearity

Utilizing the method detailed in Fig. 4 (for $z \geq 0.15$) for cooling DSC scans allows for estimation of $(\beta + x)$ values from eqn (12) and (13) with significantly higher precision than achievable with Moynihan's method, assuming the activation energy (h^*/R) or fragility m is known (Fig. 3 and 5). The error margin for the resulting $(\beta + x)$ values is typically less than 0.1. This accuracy aligns with the typical error in the nonlinearity parameter x estimated *via* the peak shift method proposed by Hutchinson,[45,46] and validated in recent extensive testing.[47] Paradoxically, the method suggested by Johari *et al.*[4] does not perform adequately for the heating scans for which it was originally proposed; the linear fit is considerably poorer and the error margins significantly exceed those of the corrected Moynihan's method.

Moynihan *et al.*[23,48] established that the glass transition temperature T_g is related to cooling rate q_c by the following equation:

$$\frac{\mathrm{d}\ln|q_c|}{\mathrm{d}(1/T_g)} = -h^*/R \qquad (14)$$

Fig. 6 displays the T_g derived from cooling scans of PVC using data from Fig. 4, plotted in accordance with eqn (14). The slope of the linear $\ln|q_c|$ *versus* $1/T_g$ plot directly yields the activation energy h^*/R. For PVC we determined h^*/R to be 225.5 ± 0.8 kK (R^2 = 0.9999), and for As_2S_3 33.37 ± 0.02 kK (R^2 = 1). These values slightly overestimate (by about 0.5–1 kK) the parameters used in TNM model calculation of cooling curves, which appears to be an inherent characteristic of eqn (14).[49] Nearly identical values are obtained for T_g' data, confirming that both linear dependences are parallel. Consequently, their differences remain constant regardless of the scanning rate: $\Delta(1000/T_g)_c$ = 0.1270 ± 0.0002 K^{-1} for PVC and 0.2676 ± 0.0001 K^{-1} for As_2S_3. By inserting these values $\Delta(1/T_g)_c$, (h^*/R) and F (for z = 0.15) into eqn (12) we estimate $(\beta + x)$ values of 0.33 for PVC and 1.08 for As_2S_3. Similarly, we can find the reduced glass transition widths: $\left(\Delta T_g/T_g'\right)_c = 0.0439 \pm 0.0003$ for PVC and 0.1153 ± 0.0059 for As_2S_3. By inserting these

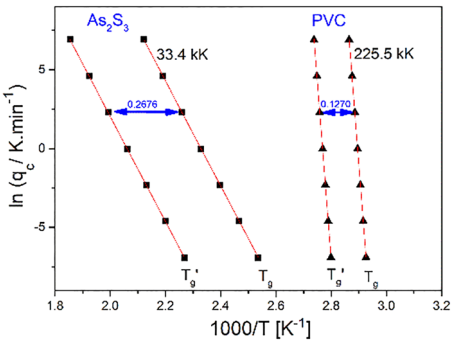

Fig. 6 Determination of the activation energy (h^*/R) and the glass transition width $\Delta(1000/T_g)_c$ using the cooling curves for PVC and As_2S_3 presented in Fig. 5.

values, fragility m and the proportionality constant F' (for $z = 0.15$) into eqn (13) we estimate $(\beta + x)$ values of 0.32 for PVC and 1.09 for As_2S_3. All calculated values exhibit good agreement with the established parameters for these materials listed in Table 1.

Combining eqn (12) and (14) yields the following relationship:

$$\beta + x = \left(\frac{F}{\ln|q_1/q_2|}\right)_{1/T} \quad (15)$$

where $\ln|q_1/q_2| = \ln|q_1| - \ln|q_2|$ is obtained at the constant value of $1000/T$, as indicated in Fig. 7b. An obvious advantage is that, according to this relationship, the sum of the parameters $(\beta + x)$ can be estimated even without explicit knowledge of the activation energy value.

Fig. 7a displays the calculated curves for various cooling rates of the $(GeTe_4)_{60}(GaTe_3)_{40}$ chalcogenide glass,[43] including the determination of the T_g and T_g' values for $z = 0.3$. Fig. 7b presents the linear dependencies $\ln|q_c|$ *versus* $1000/T$, from which $\ln|q_1|$ and $\ln|q_2|$ are determined. Linear regression of these plots yields $\ln|q_1/q_2| = 2.40$ at $1000/T = 2.4\ K^{-1}$. Using eqn (15) and the factor F corresponding to $z = 0.3$ (Table 2), an estimate of $(\beta + x) = 1.85 \pm 0.03$ is obtained, which agrees well with the parameters for this material listed in Table 1. Similarly, $\ln|q_1/q_2|$ values of 8.92 for PVC and 28.76 for As_2S_3 are estimated from the data shown in Fig. 4. Applying eqn (15) with F corresponding to $z = 0.15$, yields $(\beta + x)$ estimate of 0.32 ± 0.03 for PVC and 1.05 ± 0.03 for As_2S_3; these results closely match the values in Table 1. While the nonlinearity and nonexponentiality parameters cannot be extracted separately from the glass transition width of cooling DSC scans alone, they can easily be resolved from the temperature down-jump and up-jump experiments of the same magnitude.[50,51]

Measuring DSC cooling curves across a wide range of scanning rates can be challenging. The primary difficulty lies in achieving high cooling rates, particularly at lower temperatures. Conversely, at low cooling rates, a significant level of noise can complicate experimental data, especially for systems exhibiting only a small change in ΔC_p in the glass transition region. Given these limitations, dilatometric experiments,

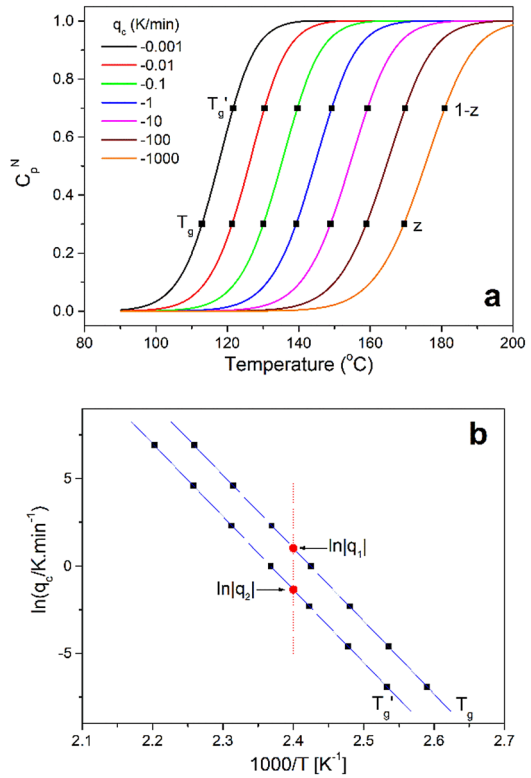

Fig. 7 (a) Determination of T_g and T_g' (at $z = 0.3$) from simulated cooling DSC scans of $(GeTe_4)_{60}(GaTe_3)_{40}$ glass at various scanning rates using TNM parameters from Table 1. (b) Evaluation of $\ln|q_1|$ and $\ln|q_2|$ at $1000/T = 2.4\ K^{-1}$ based on the cooling curves presented in Fig. 7a.

especially modern implementations like spectroscopic ellipsometry,[52] appear to be more suitable. If the glass transition cannot be reliably measured across different cooling rates, then eqn (15) is inapplicable. However, the parameter E, defined by eqn (11), remains applicable for $(\beta + x)$ estimation in a single-cooling-rate experiment if the activation energy is known. Fig. 8a illustrates the dependence of E as a function of $1/(\beta + x)$ for all materials listed in Table 1 (points corresponding to data sets shown in Fig. 4 and 7 are highlighted).

The solid lines in Fig. 8a represent the result of linear regression: $E = -0.42 + 9.61/(\beta + x)$ for $z = 0.15$ and $E = 0.47 + 3.88/(\beta + x)$ for $z = 0.30$. For a rough estimate of the nonexponentiality, the parameter C, defined by eqn (1), can be used analogously. Fig. 8b illustrates its dependence on $1/\beta$ for all materials listed in Table 1. The determination of T_g and T_g' was performed according to the numerical procedure detailed in Section 3. The solid line in Fig. 8b represents the linear regression result: $C = -3.84 + 5.57/\beta$.

In their study, Chen *et al.*[7] utilized the original Moynihan[1] graphical method with DSC experiments at a 20 K min^{-1} heating rate to determine the T_g and T_g' values for approximately 70 molecular, metallic, oxidic, and other glass-forming systems, and reported their TNM parameters. The open data points shown in Fig. 8b represent the parameter C calculated for this dataset. The linear regression $C = -4.84 + 6.59/\beta$ of

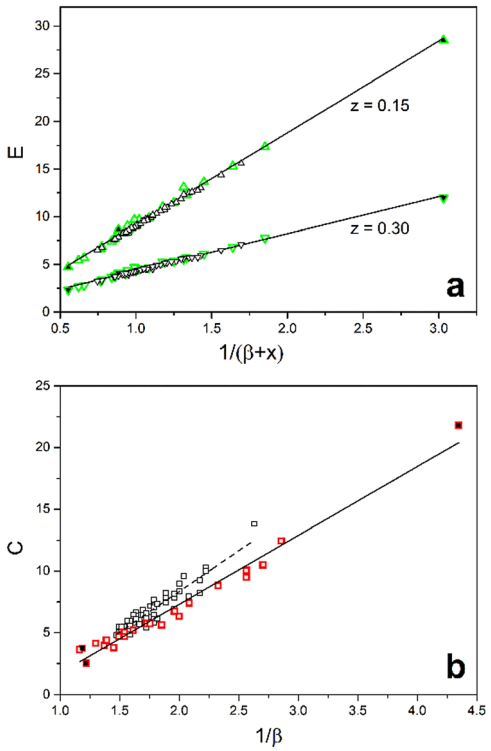

Fig. 8 (a) Dependence of the parameter E (calculated by eqn (11)) on $1/(\beta + x)$. Green points represent data for all materials listed in Table 1. Solid lines represent linear regression fits. T_g and T'_g values were determined from cooling scans using the procedure shown in Fig. 4 for $z = 0.15$ (R^2 = 0.996) and $z = 0.30$ (R^2 = 0.992). Open triangles represent data reported by Chen *et al.*[7] (b) Dependence of the parameter C (calculated by the eqn (1) using data shown in Table 1) on $1/\beta$ (red points). T_g and T'_g values were determined from heating scans according to the procedure described in Section 3. The solid line represents a linear regression fit (R^2 = 0.975). Open squares represent data and corresponding linear fit (R^2 = 0.857) extracted from Chen *et al.*[7] Highlighted points represent data sets shown in Fig. 4 and 7.

Chen's data set is weaker (R^2 = 0.857) compared to stronger correlation observed for materials in Table 1 (R^2 = 0.975). More importantly, the slope of the C *vs.* $1/\beta$ dependence is steeper compared to our dataset (dashed line, Fig. 8b). This suggests that, the specific proportionality constant C might depend slightly on the methodology used to determine T_g and T'_g values.

Chen *et al.*[7] do not provide measured cooling DSC curves; however, these curves can easily be obtained by simulation using the TNM parameters they report. In Fig. 8a, the open points represent the parameter E obtained by eqn (11), using the T_g and T'_g values determined *via* the Johari method (as described in Section 4.2, with $z = 0.15$ and 0.30, for simulated cooling curves at $q_c = -10$ K min^{-1}). The results show excellent agreement with both the data and the linear fit for all materials listed in Table 1. This demonstrates that the Johari method provides highly robust and reliably reproducible T_g and T'_g values, facilitating meaningful comparison across different materials. Consequently, the proportionality constant E remains invariant for a given value of z. In contrast, the analysis of heating scans may introduce systematic inaccuracies in the glass transition width that significantly exceed typical expectations.

5. Conclusions

The glass transition width $\Delta(1/T_g)$ or the reduced width $\Delta T_g/T'_g$ derived from DSC heating and cooling scans was comprehensively analyzed across 24 diverse materials, including inorganic glasses, organic polymers, and select molecular systems. An analysis employing the Tool-Narayanaswamy-Moynihan (TNM) model revealed significant differences between the cooling and heating processes.

The width of the glass transition during cooling scans from metastable equilibrium supercooled liquid is independent on scanning rate. Instead, it is inversely proportional to the activation energy or the fragility index m, and the sum of the nonexponentiality β and nonlinearity x parameters: $[(h^*/R) \times (\beta + x)]^{-1}$ or $[m \times (\beta + x)]^{-1}$. Notably, applying the method proposed by Johari[4] for cooling DSC scans allows for the estimation of the $(\beta + x)$ value with an accuracy comparable to that achieved *via* the established Hutchinson's peak shift method.[45,46]

In contrast the glass transition width of heating scan is influenced by both the current heating rate and the previous cooling rate. This width is inversely proportional to the activation energy or fragility, and solely the nonexponentiality parameter: $[(h^*/R) \times \beta]^{-1}$ or $[m \times \beta]^{-1}$. However, the β value estimated from the glass transition width of heating scans is considerably less accurate than the $(\beta + x)$ derived from cooling scans.

Conflicts of interest

The author declare that he has no known competing financial interests or personal relationships that could have appeared to influence the work reported in this paper.

Data availability

A significant part of the data generated during this study is included in this article and the rest of the datasets is included in supplementary information (SI) (Fig. S1–S24). Supplementary information provide simulated DSC cooling and heating scans including the fictive temperature dependences for all materials analysed and covariance and regression matrices for linear fits. See DOI: https://doi.org/10.1039/d5ma01473e.

Acknowledgements

This work was supported by the Selected Research Teams Program of the Faculty of Chemical Technology, University of Pardubice.

References

1 C. T. Moynihan, Correlation between the Width of the Glass Transition Region and the Temperature Dependence of the Viscosity of High-Tg Glasses, *J. Am. Ceram. Soc.*, 1993, **76**, 1081–1087.
2 C. T. Moynihan, K. S. Lee, M. Tatsumisago and T. Minami, Estimation of activation energies for structural relaxation and viscous flow from DTA and DSC experiments, *Thermochim. Acta*, 1996, **280/281**, 153–162.
3 K. Ito, C. T. Moynihan and C. A. Angell, Thermodynamic determination of fragility in liquids and a fragile-to-strong liquid transition in water, *Nature*, 1999, **398**, 492–495.
4 G. P. Johari, M. Beiner, C. MacDonald and J. Wang, The glass-softening temperature range and non-Arrhenius dynamics: the case of vitrified water, *J. Non-Cryst. Solids*, 2000, **278**, 58–68.
5 B. C. Hancock, C. R. Dalton, M. J. Pikal and S. L. Shamblin, A Pragmatic Test of a Simple Calorimetric Method for Determining the Fragility of Some Amorphous Pharmaceutical Materials, *Pharmaceutical Res.*, 1998, **15**, 762–767.
6 M. J. Pikal, L. Chang and X. Tang, Evaluation of Glassy-State Dynamics from the Width of the Glass Transition: Results from Theoretical Simulation of Differential Scanning Calorimetry and Comparison with Experiment, *J. Pharm. Sci.*, 2004, **93**, 981–994.
7 Z. Chen, L. Zhao, W. Tu, Z. Li, Y. Gao and L. Wang, Dependence of calorimetric glass transition profiles on relaxation dynamics in non-polymeric glass-formers, *J. Non-Cryst. Solids*, 2016, **433**, 20–27.
8 E. Bogdanova and V. Kocherbitov, Assessment of activation energy of enthalpy relaxation in sucrose-water system: effects of DSC cycle type and sample thermal history, *J. Therm. Anal. Calorim.*, 2022, **147**, 9695–9709.
9 K. Schneider, K. Schonhals and E. Donth, Uber die Grosse der kooperativen Umlagerungsbereiche am thermischen Glasubergang amorpher Polymere, *Acta Polym.*, 1981, **32**, 471–475.
10 E. Donth, The size of cooperatively rearranging regions at the glass transition, *J. Non-Cryst. Solids*, 1982, **53**, 325–330.
11 K. Hallavant, M. Mejres, J. E. K. Schawe, A. Esposito and A. Saiter-Fourcin, *J. Phys. Chem. Lett.*, 2024, **15**, 4508–4514.
12 J. E. K. Schawe, M. Kyung Kwak, M. Stoica, E. Soo Park and J. F. Loffler, *J. Phys. Chem. Lett.*, 2025, **16**, 948–954.
13 J. E. K. Schawe, K. Hallavant, A. Esposito, J. F. Loffler and A. Saiter-Fourcin, *J. Phys. Chem. Lett.*, 2025, **16**, 12255–12265.
14 A. Q. Tool, Relation between Inelastic Deformability and Thermal Expansion of Glass in its Annealing Range, *J. Am. Ceram. Soc.*, 1946, **29**, 240–253.
15 A. Q. Tool, Effect of Heat-Treatment on the Density and Constitution of High-Silica Glasses of the Borosilicate Type, *J. Am. Ceram. Soc.*, 1948, **31**, 177–186.
16 G. Adam and J. H. Gibbs, On the Temperature Dependence of Cooperative Relaxation Properties in Glass-Forming Liquids, *J. Chem. Phys.*, 1965, **43**, 139–146.
17 I. M. Hodge, Effects of Annealing and Prior History on Enthalpy Relaxation in Glassy Polymers. 6. Adam-Gibbs Formulation of Nonlinearity, *Macromolecules*, 1987, **20**, 2897–2908.
18 O. S. Narayanaswamy, A Model of Structural Relaxation in Glass, *J. Am. Ceram. Soc.*, 1971, **54**, 491–498.
19 J. C. Dyre, Narayanaswamy's 1971 aging theory and material time, *J. Chem. Phys.*, 2015, **143**, 114507.
20 I. L. Hopkins, Stress Relaxation or Creep of Linear Viscoelastic Substances under Varying Temperature, *J. Polym. Sci.*, 1958, **28**, 631–633.
21 I. M. Douglass and J. C. Dyre, Distance-as-time in physical aging, *Phys. Rev. E*, 2022, **106**, 054615.
22 O. V. Mazurin, S. M. Rekhson and Y. K. Startsev, The Role of Viscosity in the Calculation of the Properties of Glass in the Glass-Transition Region, *Fiz. Khim. Stekla*, 1975, **1**, 412–416. (English transl.).
23 C. T. Moynihan, A. J. Easteal, M. A. DeBolt and J. Tucker, Dependence of the Fictive Temperature of Glass on Cooling Rate, *J. Am. Ceram. Soc.*, 1976, **59**, 12–16.
24 M. A. DeBolt, A. J. Easteal, P. B. Macedo and C. T. Moynihan, Analysis of Structural Relaxation in Glass Using Rate Heating Data, *J. Am. Ceram. Soc.*, 1976, **59**, 16–21.
25 Y. Guo, C. Zhang, C. Lai, R. D. Priestley, M. D'Acunzi and G. Fytas, Structural Relaxation of Polymer Nanospheres under Soft and Hard Confinement: Isobaric versus Isochoric Conditions, *ACS Nano*, 2011, **5**, 5365–5373.
26 I. M. Hodge, Enthalpy relaxation and recovery in amorphous materials, *J. Non-Cryst. Solids*, 1994, **169**, 211–266.
27 Y. Han, A. D'Amore and N. Nicolais, Analysis of Structural Relaxation in a $Li_2O{\cdot}2SiO_2$ Glass using Rate Heating Approach, *J. Mater. Sci.*, 1999, **34**, 1899–1904.
28 I. M. Hodge, Effects of Annealing and Prior History on Enthalpy Relaxation in Glassy Polymers. 4. Comparison of Five Polymers, *Macromolecules*, 1983, **16**, 898–902.
29 S. L. Simon and G. B. McKenna, Interpretation of the dynamic heat capacity observed in glass-forming liquids, *J. Chem. Phys.*, 1997, **107**, 8678–8685.
30 H. Sasabe and C. T. Moynihan, Structural Relaxation in Poly(vinyl Acetate), *J. Polym. Sci.*, 1978, **16**, 1447–1457.
31 Y. P. Koh and S. L. Simon, Enthalpy Recovery of Polystyrene: Does a Long-Term Aging Plateau Exist?, *Macromolecules*, 2013, **46**, 5815–5821.
32 J. Málek, R. Svoboda, P. Pustková and P. Čičmanec, Volume and enthalpy relaxation of a-Se in the glass transition region, *J. Non-Cryst. Solids*, 2009, **355**, 264–272.
33 J. Málek and R. Svoboda, Remarkable difference in structural relaxation dynamics of conventionally prepared bulk glass and vapor-deposited thin films, *J. Chem. Phys.*, 2024, **161**, 074507.
34 G. W. Scherer, Volume relaxation far from equilibrium, *J. Am. Ceram. Soc.*, 1986, **69**, 374–381.
35 J. Málek, Dilatometric study of structural relaxation in arsenic sulfide glass, *Thermochim. Acta*, 1998, **311**, 183–198.

36 R. Svoboda, P. Honcová and J. Málek, Enthalpic structural relaxation in Se-Te glassy system, *J. Non-Cryst. Solids*, 2011, **357**, 2163–2169.
37 A. J. Easteal, J. A. Wilder, R. K. Mohr and C. T. Moynihan, Heat Capacity and Structural Relaxation of Enthalpy in As_2Se_3 Glass, *J. Am. Ceram. Soc.*, 1977, **60**, 134–138.
38 R. Svoboda, J. Málek and M. Liška, Correlation between the structure and structural relaxation data for $(GeSe_2)_y(Sb_2Se_3)_{1-y}$ glasses, *J. Non-Cryst. Solids*, 2019, **505**, 162–169.
39 R. Svoboda, J. Málek and M. Liška, Correlation between the structure and relaxation dynamics of $(GeS_2)_y(Sb_2S_3)_{1-y}$ glassy matrices, *J. Non-Cryst. Solids*, 2018, **479**, 113–119.
40 S. N. Crichton and C. T. Moynihan, Structural relaxation of lead silicate glass, *J. Non-Cryst. Solids*, 1988, **102**, 222–227.
41 S. Gaylord, B. Ananthasayanam, B. Tincher, L. Petit, C. Cox, U. Fotteringham, P. Joseph and K. Richardson, Thermal and Structural Property Characterization of Commercially Moldable Glasses, *J. Am. Ceram. Soc.*, 2010, **93**, 2207–2214.
42 R. Svoboda, M. Fraenkel, B. Frumarová, T. Wágner and J. Málek, Thermokinetic behaviour of Ag-doped $(GeS_2)_{50}(Sb_2S_3)_{50}$ glasses, *J. Non-Cryst. Solids*, 2016, **449**, 12–19.
43 R. Svoboda, M. Setnička, Z. Zmrhalová, D. Brandová and J. Málek, Structural interpretation of the enthalpy relaxation kinetics of $(GeTe_4)_y(GaTe_3)_{1-y}$ far-infrared glasses, *J. Non-Cryst. Solids*, 2016, **447**, 110–116.
44 A. M. Abd-Elnaiem and G. Abbady, A thermal analysis study of melt-quenched Zn_5Se_{95} chalcogenide glass, *J. Alloys Compd.*, 2020, **818**, 152 880.
45 J. M. Hutchinson and A. J. Kovacs, Effects of thermal history on structural recovery of glasses during isobaric heating, *Polym. Eng. Sci.*, 1984, **24**, 1087–1103.
46 J. M. Hutchinson and M. Ruddy, Thermal cycling of glasses. II. Experimental evaluation of the structure (or nonlinearity) parameter x, *J. Polym. Sci., Part B*, 1988, **26**, 2341–2366.
47 R. Svoboda, The peak-shift method for the description of structural relaxation in glassy materials: a critical review, *J. Am. Ceram. Soc.*, 2023, **106**, 5233–5247.
48 C. T. Moynihan, A. J. Easteal, J. Wilder and J. Tucker, Dependence of the Glass Transition Temperature on Heating and Cooling Rate, *J. Phys. Chem.*, 1974, **78**, 2673–2677.
49 R. Svoboda, How to determine activation energy of glass transition, *J. Therm. Anal. Calorim.*, 2014, **118**, 1721–1732.
50 J. Málek, Volume and Enthalpy Relaxation Rate in Glassy Materials, *Macromolecules*, 1998, **31**, 8312–8322.
51 J. Málek, How to Distinguish Nonexponentiality and Nonlinearity in Isothermal Structural Relaxation of Glass-Forming Materials, *J. Phys. Chem. B*, 2024, **128**, 8074–8083.
52 Y. Zhang, E. C. Glor, M. Li, T. Liu, K. Wahid, W. Zhang, R. A. Riggleman and Z. Fakhraai, Long-range correlated dynamics in ultra-thin molecular glass films, *J. Chem. Phys.*, 2016, **145**, 114502.